

## ORIGINAL ARTICLE



# Metal 3D-Printing for Repair of Steel Structures

Elyas Ghafoori<sup>1, 2, 4</sup> | Hamid Dahaghin<sup>5</sup> | Chenglei Diao<sup>2</sup> | Niels Pichler<sup>1, 3</sup> | Lingzhen Li<sup>1, 3</sup> | Jialuo Ding<sup>2</sup> | Supriyo Ganguly<sup>2</sup> | Stewart Williams<sup>2</sup>

## Correspondence

Prof. Dr. Elyas Ghafoori  
Institute for Steel Construction,  
Leibniz University Hannover  
Appelstraße 9A, 30167 Hannover  
Email: [ghafoori@stahl.uni-hannover.de](mailto:ghafoori@stahl.uni-hannover.de)

<sup>1</sup> Empa, Swiss Federal Laboratories for Materials Science and Technology, 8600 Dübendorf, Switzerland

<sup>2</sup> Welding Engineering and Laser Processing Centre, Cranfield University, Cranfield, MK430AL, UK

<sup>3</sup> ETH Zürich, Institute of Structural Engineering, 8093 Zürich, Switzerland

<sup>4</sup> Institute for Steel Construction, Leibniz University Hannover, Hannover, Germany

<sup>5</sup> School of civil engineering, University of Tehran, 16th Azar Street, Tehran, Iran

## Abstract

This work employs an innovative technique, wire arc additive manufacturing (WAAM) which is a type of directed energy deposition, for fatigue strengthening of cracked steel components. Different steel plates with a central crack were tested under high-cycle fatigue loading regime, including a reference plate, a plate repaired by WAAM with as-deposited profile, and a plate repaired by WAAM and subsequently machined to reduce stress concentration factors. Corresponding finite element simulation was conducted to provide a better understanding on the mechanism of WAAM-repair. The existing central crack in the reference plate propagated and led to a rupture after 0.94 million cycles, while those in the two WAAM-repaired plates did not propagate, due to the increased net cross-section and the compressive stresses induced by the depositing process. However, in the second plate, a new crack initiated at the root of WAAM profile as a result of local stress concentration, and the fatigue life reached 2.2 million cycles (2.3 times as the reference plate). The third plate, on the other hand, survived more than 9 million fatigue cycles with no visible degradation, thanks to its smooth machined profile. The findings of this work indicate that WAAM repair shows great potential as a technique to address fatigue-related damages in steel structures.

## Keywords

Directed energy deposition, fatigue strengthening, 3D-printing, crack arrest, fatigue life extension

## 1 Introduction

Metallic structures subjected fatigue loading, e.g., steel bridges and steel cranes, are prone to fatigue damage, which degrades the mechanical performance of steel structures. Several techniques exist to combat the fatigue problems of steel structures, for instance, impact crack closure retrofit treatment [1], unbonded/bonded CFRP strengthening [2], and unbonded/bonded Fe-SMA strengthening [3][5]. The main mechanism for fatigue strengthening is to reduce the local stress concentration at the crack tip typically by: (1) introducing extra stress transferring paths and (2) introducing compression to the cracked section.

In this study, an innovative technique, WAAM (also known as 3D-printing metal), is used to solve the fatigue problem of steel structures. The process of WAAM repair is to deposit melted steel wire onto the target area in a steel substrate and waiting until it cools down to the room temperature. Two main benefits will be discussed in the following: (1) the local stress is reduced as a result of increased net cross-section (deposited steel material), and (2) compressive stress can be generated during the cooling process

provided that the deposition path is well designed. To investigate the efficacy of the WAAM repair, three fatigue tests were conducted in this study: (1) a reference plate without any repair/strengthening; (2) a plate repaired by WAAM with as-deposited profile, and (3) a plate repaired by WAAM, which was subsequently machined to a pyramid profile to reduce the stress concentration at the deposition root. FE simulation of these three plates was conducted to assist explaining the experimental results and understanding the mechanisms of the WAAM repair.

## 2 Methods

To assess the effectiveness of the proposed strengthening system, two fatigue tests were conducted on the WAAM-repaired steel plates. The specimens used were mild steel plates of grade S355J2+N with a central notch cut by electrical discharge machining (EDM), as presented in Figure 1. The same specimen configuration was used in studies [3]–[5] to investigate other strengthening strategies. The steel plates have a yield strength of 421 MPa, an ultimate tensile strength of 526 MPa, and an elastic modulus of 205 GPa [4].

## 2.1 Initial damage by precracking

Residual stress stem from the EDM machining of the notch shown in Figure 1. Therefore, the plates are precracked to eliminate the effects of the machining on the crack tip and create a sharp crack tip. The plates were subjected to 100,000 cycles with  $\Delta\sigma=75$  MPa and  $R=0.2$  to propagate the half crack length from 7.5 to approximately 8.5 mm. The plates were subsequently strengthened.

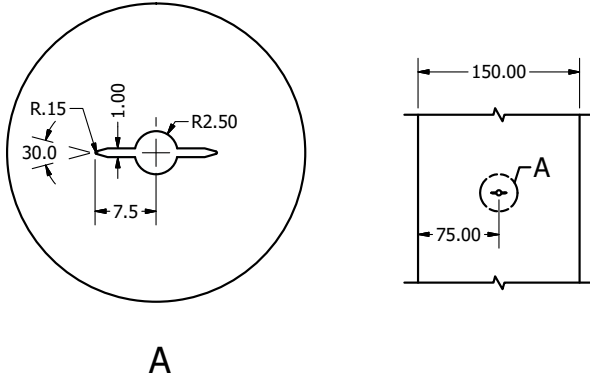


**Figure 1** Details of the specimen before precracking and repair, total specimen length was 850 mm and thickness 10mm.

## 2.2 WAAM repair

The WAAM deposition experimental setup can be found in Figure 2. It included a Kuka 6-axis industrial robot with a MTB500 Cold Metal Transfer (CMT) torch and Fronius power supply.

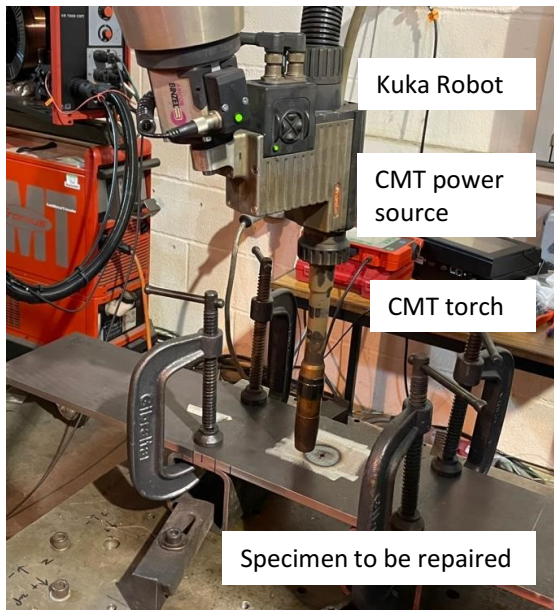


**Figure 2** The setup for strengthening using WAAM.

CMT was chosen for the deposition process as it reduces the heat input and minimises the distortion. The deposition is conducted at a constant starting temperature for each layer and alternated the deposition sides between the top and bottom surface every layer to reduce potential distortion. The specimen plate was finished to ensure perfect bonding between the WAAM deposited material and the original plate. The process parameters can be found in the Table 1 below:

**Table 1** Process parameters

Process	CMT
Synergic line	CMT 1355 with 1.0mm wire
Gas	Pureshield Argon + CO2
Wire	ER90
Arc length correction	0%
Wire feed speed	5.8 m/min
Travel speed	10 mm/s
Bead Width	4.8 mm
In process temperature	20 °C

The repairs consisted of a square patch of 30 by 30 mm and 8 mm thick deposited on each side of the plate centered on the initially machined notch. The result of the depositing process can be seen in Figure 3 (a) and (c). Since the depositing process is similar to the welding, which potentially induces new fatigue problems due to the stress concentration and residual stress etc., one of the repairs was machined to a pyramid like shape (Figure 3(b) and (d)) in order to reduce the stress concentrations at the depositing root.

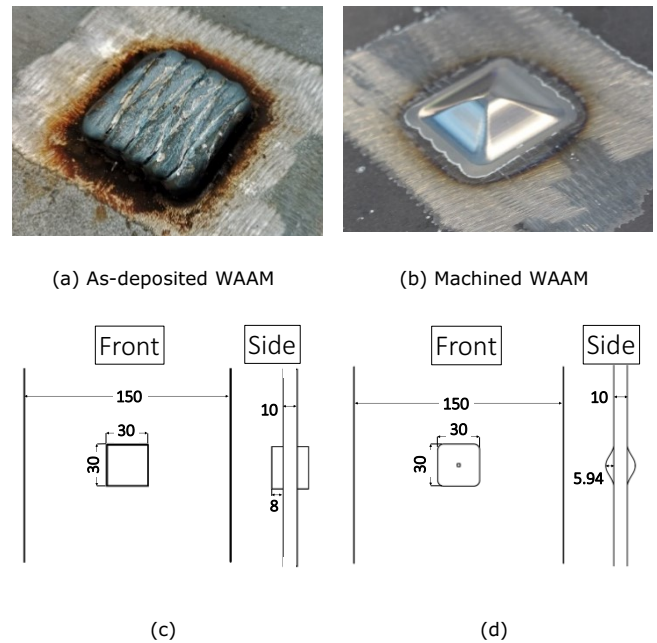


**Figure 3** Geometry of steel plate repaired with WAAM. (a, c). As-deposited, (b, d) Machined (in mm)

## 2.3 Static and fatigue experiments

To investigate the strengthening efficacy, fatigue tests were conducted on all the specimens. Prior to the fatigue tests, a static test was carried out on the machined sample, to better understand the mechanism of WAAM strengthening and validate the finite element (FE) model via strain field comparison. The plate with machined WAAM repair was tensioned to 100 kN (nominal tensile stress was 66.7 MPa) under load control and then unloaded to zero force without any expected damage to the plate. The loading rate was 0.5 kN/s, and the sampling

rate was 5 Hz; a 3D digital image correlation (DIC) technique was utilized to measure the full-field strain, with an image acquisition rate of 1 Hz. Both the static and fatigue tests were conducted in a servo-hydraulic testing machine (Walter & Bai) with a maximum capacity of 500 kN. The test and measurement setups are shown in Figure 4.

Fatigue tests of the two WAAM-repaired plates were conducted under load control. The maximum and minimum tensile stress on the nominal cross-section are 93.75 MPa and 18.75 MPa, respectively, with a stress range of 75 MPa, a stress ratio (R ratio) of 0.2, and a frequency of 10 Hz. For tracking the crack length and the corresponding fatigue loading cycles, a beach-marking loading regime, with an increased R ratio of 0.6, was used; the minimum nominal stress became 56.25 MPa, while the maximum nominal stress was kept unchanged.

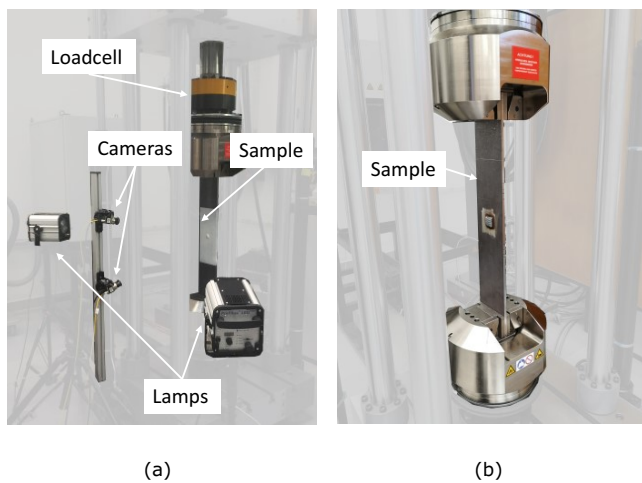


**Figure 4** Experimental setups. (a) Static test with 3D DIC measurement, (b) Fatigue test setup.

## 2.4 Finite element modelling of WAAM repair

In order to have deeper insight into the mechanism of the WAAM strengthening, the three plates, i.e., a reference plate, an as-deposited WAAM repaired plate, and a machined WAAM repaired plate, were modelled using FE software ABAQUS 2017 [6]. In this study, a fast simulation approach, comprising the inherent strain (IS) technique as a computationally efficient method, was adopted to predict the residual stresses introduced during the WAAM process. The IS technique was applied and validated in the simulation of large welded structures [7]–[12], which have very similar process as the WAAM repair.

The geometries, dimensions, and mechanical properties used in the FE models were the same as those used in the experiment. Moreover, the same mechanical properties were considered for WAAM material in both as-deposited and machined WAAM repaired specimens. Due to the geometrical symmetry, only one-eighth of the samples were modeled as shown in Figure 5. Most elements in the steel plate and as-deposited WAAM elements were defined as C3D8R elements, while C3D6 elements were used to model the wedge elements around crack tip with very fine radial mesh, as depicted in Figure 5. In addition, the machined WAAM (the pyramid-like) detail was modelled by C3D10 elements. The interface between WAAM and the steel plate in both models was considered as “tie”. The crack was modeled in ABAQUS by defining crack tip and

crack extension direction. A uniformly distributed tensile pressure,  $\sigma$ , as shown in Figure 5, was applied at the two ends of the steel plate.

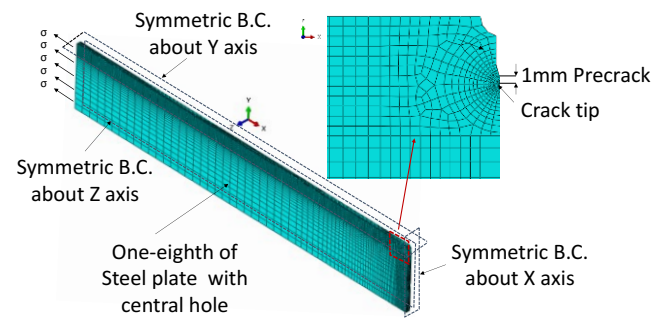


**Figure 5** Model, boundary conditions and mesh of the reference sample in ABAQUS

The stress intensity factor (SIF) at the crack tip of the reference plate obtained via J-integral was compared with that estimated from Equation (1) to validate the FE model. In Equation (1),  $a$  and  $w$  are the half crack length and width of the specimen respectively. A good agreement is found as the two approach deviate only 2.85 as shown in Table 2.

$$K_I = \sqrt{\sec\left(\frac{\pi a}{w}\right)} \cdot \sigma \cdot \sqrt{\pi a} \quad (1)$$

**Table 2** SIF comparison

SIF <sub>Analytical</sub> (N/mm <sup>3/2</sup> )	SIF <sub>FEM</sub> (N/mm <sup>3/2</sup> )	Error (%)
488.24	502.35	2.8

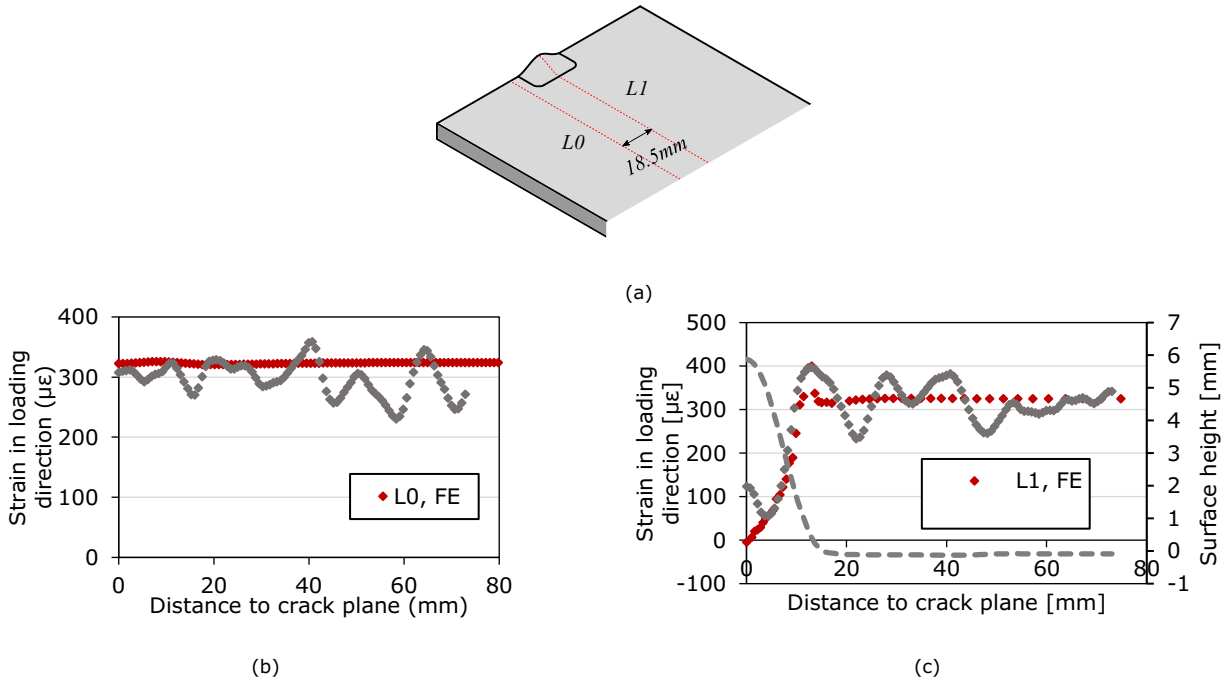
## 3 Results and Discussion

### 3.1 Static test and strain measurement

Figure 6 shows a comparison between the experimentally measured strain using DIC and the computed strain in the FE model at the end of the static loading of the machined plate, with a tensile force of 99.6kN. Figure 6 (a) displays the two lines on the sample surface, on which the strains were extracted for analysis; a centreline (L1) passes through the middle of the deposited strengthening, and a reference line (L0) locates 18.5 mm away from the centreline. The strain profile in the loading direction along L0 and L1 are displayed in Figure 6 (b) and Figure 6 (c), respectively. A general agreement was observed between the experimentally measured and FE computed strain on these two lines, suggesting that the IS technique and the selected elements are appropriate to model the WAAM repaired steel member. The slight fluctuations in the experimental results are within the range of the noise of the DIC technique.

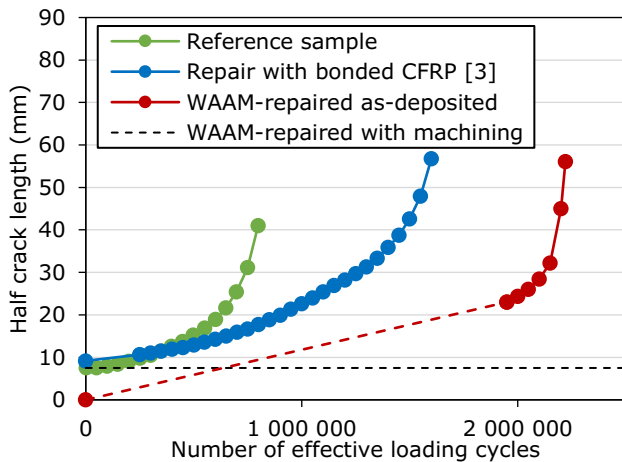
### 3.2 Fatigue tests

Figure 7 shows the fatigue tests results in the form of a-N curves, half crack length vs. fatigue loading numbers. Four specimens are used: a reference plate [3] and the two WAAM-repaired plates tested in the current study. Additionally, in order to compare the efficiency of the proposed



**Figure 6** Comparison between experimental strain measured by DIC and strain computed by FE modelling under an applied load of 99.6kN. (a) Location of L0 and L1. (b) Strain profile 18.5 mm away from the middle of the sample. (c) Strain profile on L1, passing through the repair.

repair technique with the conventional repair using composite materials, the results of repair using bonded carbon fibre reinforced polymer (CFRP) strips [3] were also depicted.



**Figure 7** a-N curves of fatigue specimens. Machined WAAM repair specimen is not shown in this figure, since no sign of fatigue damage is shown after 6 million fatigue cycles and 3 more million cycles at 20% increased load level.

The bonded strengthening with (non-prestressed) bonded CFRP strips reduces the stress intensity at the crack tip by introducing extra stress transferring paths, hence, retarding the crack propagation speed. In the end, the fatigue life was enhanced from 0.94 million to 1.6 million. While the life extension is considerable, this result needs to be considered with caution due to the limited amount of results. When WAAM repair is used, no crack propagation was observed from the existing crack. However, a new crack initiated at the edge of the front WAAM profile (deposition root), as shown in Figure 8, and the final fatigue life was 2.22 million cycles. For the machined specimens, neither fatigue crack propagation of existing crack nor new

crack initiation at the depositing root was observed after 6 million effective cycles. The authors further increased the fatigue load level by 20% (maximum and minimum nominal stress are 112.5 MPa and 22.5 MPa, respectively), and the fatigue test ran 3 million more effective cycles. Again, no sign of fatigue damage was observed. It can be then concluded that the crack propagation of existing crack is fully arrested, however, there is a chance of new crack initiation at the interface between the WAAM profile and the steel substrate. The risk for formation of this new fatigue crack initiation can, however, be reduced by machining the deposited WAAM detail to provide a smooth transition.

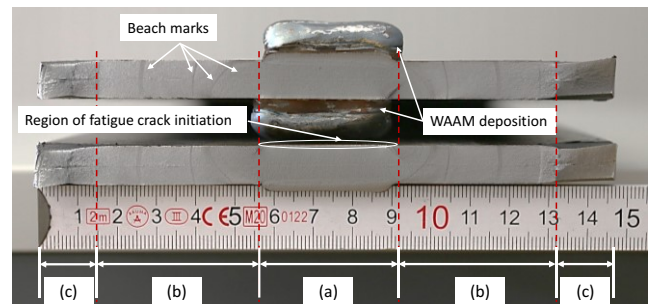


**Figure 8** Fracture surface of as-deposited WAAM repair specimen with three regions: (a) fatigue crack initiation and through thickness propagation, (b) crack propagation through the width direction, and (c) brittle rupture.

### 3.3 FE simulations and discussions

The aim of the FE modeling in this study is to investigate and understand the effect of WAAM repair on fatigue crack retardation and arrest. Figure 9 (a) and (b) show the simulated longitudinal residual stresses of as-deposited and machined WAAM samples, respectively, prior to any loading. The tensile residual stress was generated during the cooling process with WAAM solidification. These stress-

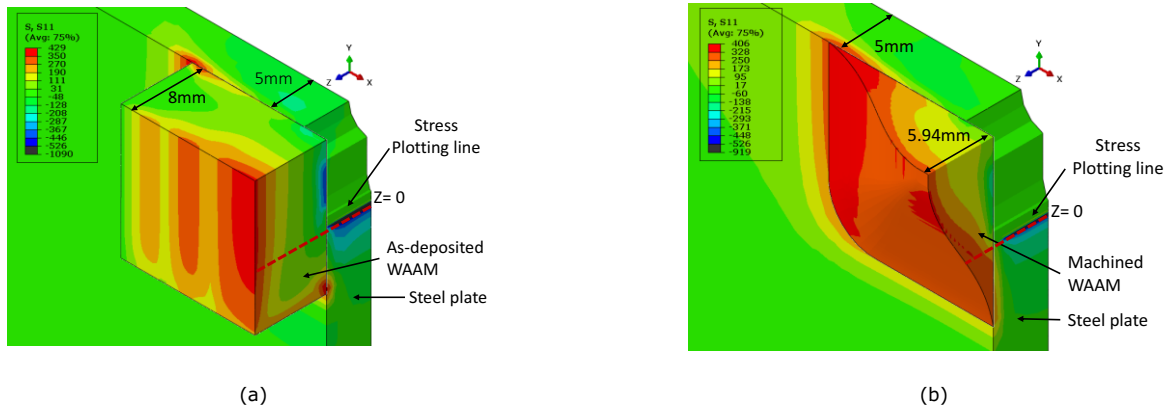


**Figure 9** Longitudinal residual stress distribution due to WAAM process (in MPa). (a) Steel plate repaired with as-deposited, WAAM (b) Steel plate repaired with machined WAAM.

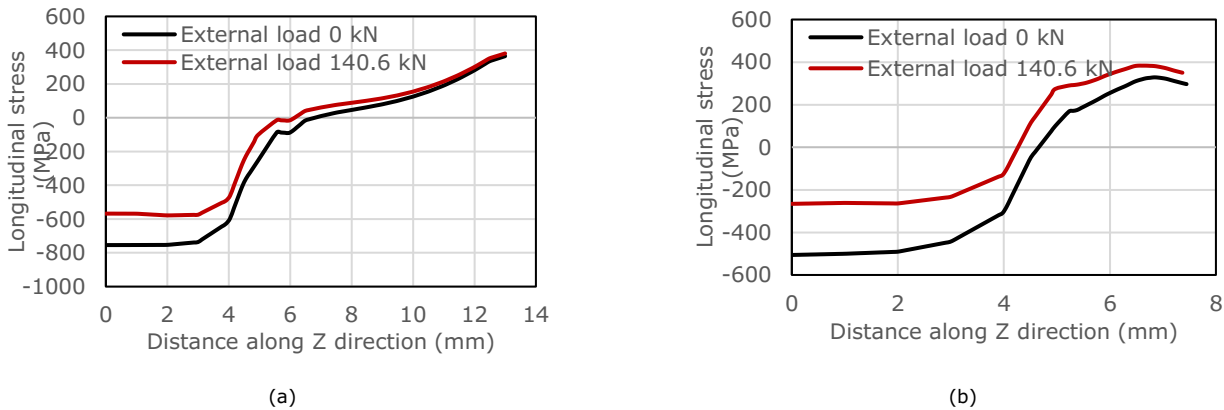


**Figure 10** Longitudinal stress along the dotted lines in Figure 9 before and after loading. (a) Steel plate repaired with as-deposited WAAM, (b) Steel plate repaired with machined WAAM

es induced a balancing compressive stress in the steel plate and especially around the crack tip as shown in Figure 10 (a) and (b). Figure 10 (a) and (b) depict the longitudinal stresses at the locations of the red dashed lines in Figure 9 (a) and (b) of the two WAAM repaired plates. The blue solid curves show the stress state prior to external loading (after applying WAAM repair), while the orange dashed curves depict the stress state after applying the external load. It is clearly seen that due to the WAAM repair, the crack tips were brought to the compressive side, and the external load applied in the current study could not open the crack tip. This is the reason that no crack propagation of the existing crack was observed in these two plates during the fatigue tests.

Figure 11 depicts the computed SIF against the applied load of the three plates. Note here, the negative values of the SIFs, though lacking physical meaning, demonstrate the absence of the crack driving force. Similar results can be found in [4]. For these WAAM repaired plates, their crack tips are under compression during the whole fatigue loading process, with applied load ranging from 28.1 – 168.7 kN. This further explains the fatigue crack arrest phenomenon for the existing crack. Moreover, some similarity was found between WAAM repair and the prestressed strengthening using CFRP strips [3], [4], [13] and iron-based shape memory alloy (Fe-SMA) strips [2] [3], as they all introduce compression in the steel plate around the crack tip and bring extra stress transferring paths.

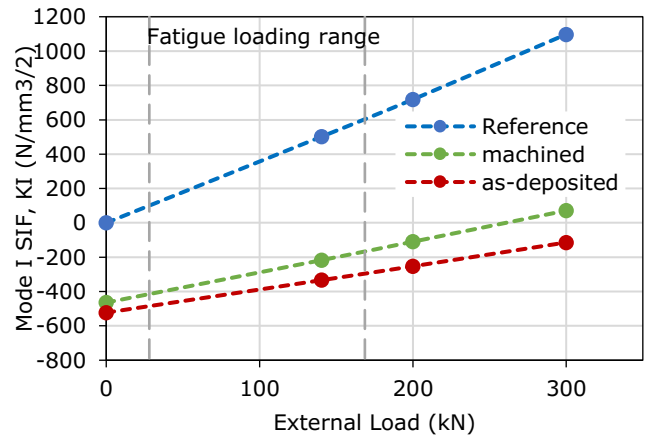


**Figure 11** Magnitude of the stress intensity factors for the reference and repaired samples as function of the applied load

Although the WAAM induced compression prevented the existing crack tips from propagation, the high stress level at the welding root would lead to a new problem: fatigue crack initiation from the WAAM-steel interface. Figure 12 shows the longitudinal stress in steel plate for as-deposited and machined WAAM samples. Due to the geometrical discontinuity and the cooling contraction during the WAAM process, a high stress level close to the yielding stress is observed at the depositing root, see Figure 12 (a). In the end, new fatigue crack initiated at the depositing root under fatigue loading, and this finally led to the failure of the plate. By machining the WAAM details to a pyramid shape, the stress level at the depositing root was reduced from 422 to 258 MPa, which is approximately half of that with the as-deposited WAAM details. After 6 million cycles and

3 million cycles with increased load level, no sign of crack initiation was observed, which means the machined WAAM-repair has not only arrested the existing crack but also prevented a new crack initiation.

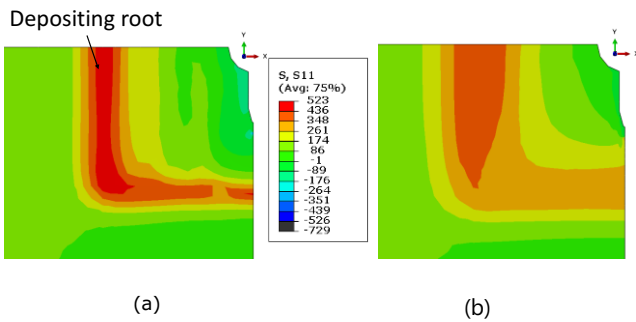


**Figure 12** Stress distribution in steel plate after loading (in MPa). (a) Steel plate repaired with as-deposited WAAM, (b) steel plate repaired with machined WAAM

#### 4 Conclusion

In the current study, WAAM technique was used for fatigue strengthening of damaged steel plates. Two cracked steel plates with two strategies, i.e., as-deposited and machined WAAM repairs, were tested under static load and fatigue load. FE simulation was conducted to reveal the mechanism of WAAM repair. The following conclusions can be drawn:

1. The WAAM repair reduces the stress concentration at the existing crack tips by introducing extra stress transfer paths and generating a compressive stress field in the steel substrate. At the end, the crack did not propagate from the existing crack in both WAAM-repaired samples. The mechanism has an analogy with the prestressed strengthening using CFRP and Fe-SMA strips.
2. The WAAM details induce geometrical discontinuity and generate stress concentration, which may lead to new crack initiation and eventually limited fatigue life.
3. Machining the WAAM-repaired details provides a smooth geometrical change and dramatically reduces the stress concentration at the hotspots to ensure no new fatigue crack is formed at the WAAM-to-steel interface.

#### Acknowledgement

The support provided by the Swiss National Science Foundation (SNSF) with a project number IZSEZ0\_202441 for this work is acknowledged.

#### References

- [1] Y. Kentaro, I. Toshiyuki, and K. Takumi, "REHABILITATION AND IMPROVEMENT OF FATIGUE LIFE OF WELDED JOINTS BY ICR TREATMENT," *Advanced Steel Construction*, vol. 11, no. 3, pp. 294–304, 2015, doi: 10.18057/IJASC.2015.11.3.
- [2] A. Hosseini et al., "Development of prestressed unbonded and bonded CFRP strengthening solutions for tensile metallic members," *Engineering Structures*, vol. 181, pp. 550–561, Feb. 2019, doi: 10.1016/j.engstruct.2018.12.020.
- [3] W. Wang, L. Li, A. Hosseini, and E. Ghafoori, "Novel fatigue strengthening solution for metallic structures using adhesively bonded Fe-SMA strips: A proof of concept study," *International Journal of Fatigue*, vol. 148, p. 106237, Jul. 2021, doi: 10.1016/j.ijfatigue.2021.106237.
- [4] A. Hosseini, E. Ghafoori, M. Motavalli, A. Nussbaumer, and X.-L. Zhao, "Mode I fatigue crack arrest in tensile steel members using prestressed CFRP plates," *Composite Structures*, vol. 178, pp. 119–134, Oct. 2017, doi: 10.1016/j.compstruct.2017.06.056.
- [5] M. R. Izadi, E. Ghafoori, M. Motavalli, and S. Maalek, "Iron-based shape memory alloy for the fatigue strengthening of cracked steel plates: Effects of re-activations and loading frequencies," *Engineering Structures*, vol. 176, pp. 953–967, Dec. 2018, doi: 10.1016/j.engstruct.2018.09.021.
- [6] M. Smith, "ABAQUS/Standard User's Manual, Version 6.14." Dassault Systèmes Simulia Corp, 2017.
- [7] Hill, M. R., & Nelson, D. V. (1995). The inherent strain method for residual stress determination and its application to a long welded joint. *ASME-PUBLICATIONS-PVP*, 318, 343–352.
- [8] Y. Luo, H. Murakawa, and Y. Ueda, "Prediction of Welding Deformation and Residual Stress by Elastic FEM Based on Inherent Strain," *J. SNAJ, Nihon zousen gakkai ronbunshu*, vol. 1997, no. 182, pp. 783–793, 1997, doi: 10.2534/jjasnaoe1968.1997.182\_783.
- [9] D. Deng, H. Murakawa, and W. Liang, "Numerical simulation of welding distortion in large structures," *Computer Methods in Applied Mechanics and Engineering*, vol. 196, no. 45–48, pp. 4613–4627, Sep. 2007, doi: 10.1016/j.cma.2007.05.023.
- [10] D. Deng and H. Murakawa, "Prediction of welding distortion and residual stress in a thin plate butt-welded joint," *Computational Materials Science*, vol. 43, no. 2, pp. 353–365, Aug. 2008, doi: 10.1016/j.com-matsci.2007.12.006.
- [11] R. Wang, J. Zhang, H. Serizawa, and H. Murakawa, "Study of welding inherent deformations in thin plates based on finite element analysis using interactive substructure method," *Materials & Design*, vol. 30, no. 9, pp. 3474–3481, Oct. 2009, doi: 10.1016/j.matdes.2009.03.015.
- [12] X. Liang, Q. Chen, L. Cheng, D. Hayduke, and A. C. To, "Modified inherent strain method for efficient prediction of residual deformation in direct metal laser sintered components," *Comput Mech*, vol. 64, no. 6, pp. 1719–1733, Dec. 2019, doi: 10.1007/s00466-019-01748-6.
- [13] E. Ghafoori, M. Motavalli, J. Botsis, A. Herwig, and M. Galli, "Fatigue strengthening of damaged metallic beams using prestressed unbonded and bonded CFRP plates," *International Journal of Fatigue*, vol. 44, pp. 303–315, Nov. 2012, doi: 10.1016/j.ijfatigue.2012.03.006.

# Metal 3D-printing for repair of steel structures

Ghafoori, Elyas

2023-09-12

Attribution 4.0 International

---

Ghafoori E, Dahaghin H, Diao C, et al., (2023) Metal 3D-printing for repair of steel structures. In: 10th Eurosteel Conference, 12-14 September 2023, Amsterdam, The Netherlands

<https://doi.org/10.1002/cepa.2285>

*Downloaded from CERES Research Repository, Cranfield University*